Mitigation of Superconducting AC Losses in Axial Flux Synchronous Machines With Multifilament Coated Superconductors

2LPo2F-02

Mitigation of Superconducting AC Losses in Axial Flux Synchronous Machines with Multifilament Coated Superconductors

Inês S.P. Peixoto, *Student Member, IEEE*, Yusuke Sogabe *Member, IEEE*, João F. P. Fernandes *Member, IEEE*, Silvio Vaschetto *Senior Member, IEEE* and Naoyuki Amemiya *Senior Member, IEEE*

***Abstract*—Fully superconducting machine typologies allow maximizing the advantages of superconductors in rotating electrical machines and might be a key in overcoming the power density limitations of current technologies. However, their realization is facing a challenge since superconductors generate non negligible AC losses when supplied by AC currents or subjected to AC fields. Deviating the magnetic field from the wide surface of the conductor and striation are proven methods to significantly reduce magnetization losses in coated conductors. However, striation is only effective when filaments are decoupled electromagnetically. Winding a copper-plated striated coated conductor spirally around a core is a novel method to decouple filaments. In this work, cables consisting of such multifilament coated conductors are applied in an axial flux synchronous machine model and their losses are compared to those of superconducting tapes with magnetic leakage flux parallel to their wide surfaces. Cables' models are first verified by comparison with analytical and experimental results. Then, these are applied in a single slot model previously developed by the authors to analyze and compare loss results to those of single tapes carrying the same current when exposed to the same surrounding magnetic fields.**

***Index Terms*— AC loss, finite element method, SCSC cable, Superconducting machines, *T-A* formulation.**

I. Introduction

THE use of superconductors (SCs), with their high current carrying capacity might lead to increased magnetic loading and reduced weight in electrical machines [1]–[3]. However, present-day technology in superconducting tapes and cables still faces limitations, such as the non-negligible superconducting loss in AC conditions and material strain/bending limitations [4], [5]. The reduction of superconductor AC loss can be achieved through machine design and superconductor structural modifications [6]. Introducing ferromagnetic materials in the vicinity of the superconductor and strategic coil positioning can help mitigate the impact of external magnetic field on SCs ensuring the field is mostly parallel to the superconductors flat surface [7] – [11].

From a structural perspective, the striation of tapes allows for a reduction in magnetization losses, which are proportional to the conductor width [12] – [15]. However, if a local quench occurs in one of the filaments, an alternative current path is necessary for stable operation. Current sharing between filaments (and increased reliability against quench) can be achieved by copper plating the multifilament tape [16]. Yet, once the filaments are electrically connected, electromagnetic coupling can make the multifilament structure ineffective for loss reduction [17]. To decouple the filaments, the striated tapes must be spirally wound around a core at short twist pitches, to reduce coupling currents decay time [18], [19]. While the Spiral Copper-plated Striated Coated conductor (SCSC) cable stability against quench is provided by the tapes' copper plating and the cable's conducting core. Its low loss at operating frequencies up to few kHz is granted by the spiral geometry. Both characteristics make the cables appropriate for application in electrical machines armature windings where they are exposed to alternate fields and currents.

Regarding their mechanical limitations, SC tapes can only be bent over their widest face with strict bending restrictions. This means that when inserted in electrical machines, specific winding topologies (e.g., distributed windings) become hardly realizable. Conversely, superconducting cables can be bent in all directions despite their minimum bending radius. In addition, the losses in superconducting cables are unaffected by the direction of the surrounding magnetic field. This means that due to the cable's twisted geometry, changes of magnetic field direction in end-winding regions would have minimal impact in superconducting losses.

This paper proposes a methodology to estimate AC performance of SCSC cables in axial flux electrical machine armature windings using finite element method (FEM) tools. To

This work was supported by JST-ALCA-Next Program Grant Number JPMJAN24G1 (JST-Mirai Program Grant Number JPMJMI19E1), Japan. The research activities developed by Inês S. P. Peixoto have been conducted in the frame of the Doctoral Research programme funded by the Italian Ministry of University and Research through the Operative National Program (PON) for Research and Innovation 2014-2020, M.D. 1061 (10 Aug. 2021), Action IV.5 "Ph.D. programmes on sustainability-based topics". (Corresponding author: Yusuke Sogabe)

I.S.P. Peixoto and S. Vaschetto, are with the Politecnico di Torino, Dipartimento Energia "G. Ferraris", Torino, 10129, Italy (e-mail: ines.peixoto@polito.it, silvio.vaschetto@polito.it).

Y. Sogabe and N. Amemiya are with the Department of Electrical Engineering, Kyoto University, Kyoto 615-8510, Japan (e-mail: sogabe.yusuke.6s@kyoto-u.ac.jp, amemiya.naoyuki.6a@kyoto-u.ac.jp).

J.F.P. Fernandes is with Departamento de Engenharia Electrotécnica e de Computadores, University of Lisbon, Instituto Superior Técnico, Lisbon Portugal (e-mail: joao.f.p.fernandes@tecnico.ulisboa.pt)

Color versions of one or more of the figures in this article are available online at http://ieeexplore.ieee.org

estimate losses in SC elements, a high level of detail is imperative to guarantee precise results. This makes FEM models computationally demanding and time consuming, especially when 3D geometries are required such as in axial flux permanent magnet (AFPM) machines. Several formulations are reported in literature that allow describing superconductors using their characteristic non-linear resistivity power law and their dependence on surrounding magnetic fields [20]. Nonetheless, expedite methods to evaluate the performance of superconducting electrical machines are still scarce. In [21] a 2D model was proposed for faster SC loss analyses in superconducting armature windings. This model is constructed by acquiring, from a 3D electrical machine simulation, the first harmonic of the magnetic field surrounding the superconductors along the armature slot borders. In this study, the model in [21] is expanded to include a full description of the magnetic field harmonics surrounding the SCs and used to analyze the SCSC cables' losses and compare them to those of REBCO tapes.

II. SCSC Cable Modelling

Due to the high aspect ratio of 2nd generation superconducting tapes, it is possible to assume that current flows in the superconducting layer tangentially to the tape surface [22], [23]. This means that the *T-A* formulation with the thin sheet approximation can be applied allowing a significant reduction of computational complexity of the model, by reducing the number of degrees of freedom of the HTS domain [20]. The SC dependence on the applied magnetic field and its characteristic resistivity are defined in FEM by the Kim model in (1) and the *E-J* power law in (2) [24], [25].

$$J_c(\mathbf{B}) = J_{c0}\frac{1}{1+|\mathbf{B}|/B_0} \tag{1}$$

In (1) J_{c0} is the critical current density at self-field, and B_0 the magnetic field that lowers the critical current density J_c by half.

$$\mathbf{E} = E_0\left(\frac{|\mathbf{J}|}{J_c(\mathbf{B})}\right)^{(n-1)}\frac{\mathbf{J}}{J_c(\mathbf{B})} \tag{2}$$

In (2) E_0 is the critical electric field, defined by convention as 100 μV/m, and n is the superconducting exponential constant which defines the steepness of the transition between the superconducting and resistive state.

A. The T-A formulation

The numerical model is constructed by defining in the tape domain, Ω_{SC}, the potential vector **T**, and in all other domains Ω_A the magnetic vector potential **A**, as in (3). Through the defined relations, Faraday's law can then be solved in FEM (4) [26].

$$\nabla\times\mathbf{T}=\mathbf{J}\text{ in }\Omega_{SC}\qquad \nabla\times\mathbf{A}=\mathbf{B}\text{ in }\Omega_A \tag{3}$$

$$\nabla\times\mathbf{E}=-\partial\mathbf{B}/\partial t \tag{4}$$

Current is applied in the tapes by imposing Dirichlet boundary conditions at its edges. The value for T at each edge of the tape $T_1 = 0$ and $T_2 = I/\delta$ is obtained by integrating **J** over the cross-section of the layer as in (5) [27].

$$\iint_S \mathbf{J}\cdot\mathbf{n}dS = \oint_L \mathbf{T}\cdot dl = (T_1 - T_2)\delta \tag{5}$$

TABLE I
Striated Coated Conductor And REBCO Parameters

Parameter	Striated coated conductor	REBCO tape
I_c* (A)	35	162
B_0* (mT)	150	150
n*	21	21
Tape width (mm)	2	4
Number of SC filaments	10	1
Width of filaments (mm)	0.155	-
Copper width (μm)	50	-
Tape thickness (μm)	95.6	95.6

*Measured at 77 K

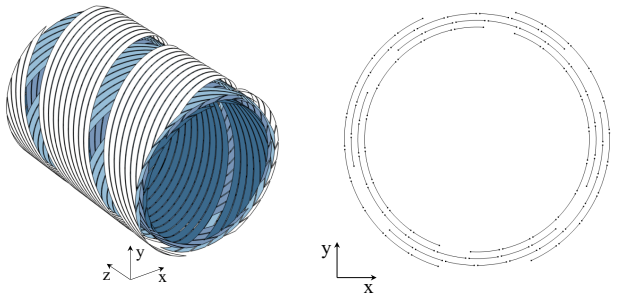

(a) (b)

Fig. 1. Illustration of one pitch of the SCSC cable, modelled by the thin sheet approximation in 3D (a) and 2D models (b).

In (5) L denotes the path formed by the boundary edges of the conductor, and δ is the thickness of the superconductor. In this study, constant temperature operation at 77 K was assumed for all models.

B. 3D and 2D model for magnetization loss estimation

The specifications of the multifilament coated conductor, and the REBCO tape are stated in Table I [21], [28]. The considered SCSC cable has two tapes per layer and a total of four layers of striated coated conductors. The cable core diameter, D_c, and its twist pitch, L_p, are 3 mm and 4.7 mm respectively.

The focus of this work is to present a methodology for SCSC cable loss estimation in armature windings, thus, cables found suitable for a test setup were considered in this study. For the practical realization of superconducting armature windings, SCSC cables with tapes of increased critical currents and higher number of filaments would be a more suitable choice.

The geometry of one pitch of the cable is shown in Fig. 1a. Here, only superconducting filaments are modeled, since the operating conditions allow assuming the current flows mainly in the SC layers. The 2D cable geometry, shown in Fig.1b, corresponds to a cross section of the 3D model, through a plane normal to the cable axial direction (z-axis in Fig 1a).

In Fig. 2 a SC filament is depicted with the 2D model variables. Note that the current defined in the 2D model, $\mathbf{J_z}$, is perpendicular to the model plane. Furthermore, the tapes' width is increased by a factor of 1/cos(θ), where θ is the angle between the coated conductor and the cable axis ($\theta = 64^o$). This means that the considered critical current in the 2D model must also be increased by the same factor, hence, I_{c2D} becomes $I_c/\cos(\theta)$.

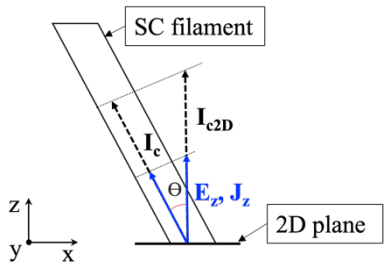

Fig. 2. Illustration of one filament of the SCSC cable with representation of the considered variables.

Similarly, the computed variables **E** and **J** used to evaluate the losses must be corrected by a factor of cos(θ).

The *T-A* formulation is applied in FEM to both 2D and 3D models, to estimate the cable's AC loss with an externally applied alternate magnetic field $H_m(t) = H_0 \sin(\omega t+\phi)$, in the *y*- axis direction. For the magnetization loss simulation both values of T_1 and T_2 are defined as zero. The considered magnetic field amplitude is varied between 10 mT and 100 mT and its frequency *f* is set as 112Hz in agreement with results in [28]. Note that since the considered cables measured coupling time constant, $\tau_c = 1/2\pi f_c$, is 0.05 ms the characteristic frequency f_c, above which filaments are coupled is 3183Hz [28]. This means the filaments remain uncoupled for the considered operating conditions in this study, making cable losses mostly hysteretic [29]. In this situation, loss estimation in 2D, i.e., without representing the twisted geometry, provides results close to those obtained in 3D models.

The current distribution is plotted for both models in Fig. 3 for a magnetic field amplitude B_m of 100 mT. Since the 2D and the 3D models' current density profiles agree, and *E-J* parameters are the same, then the losses must also agree. The magnetization losses (per cable meter) for different values magnetic field amplitude are shown in Fig. 4. with the experimental results reported in [28]. Analytical results for magnetization losses for SC tapes under applied transverse magnetic field, Q_{BI} (6) are also shown for comparison [30].

$$Q_{BI} = \mu_0 w^2 f J_c \delta H_0 g\left(\frac{H_0}{H_c}\right) \quad (6)$$

In (6) *w* is the superconductor filament width, and H_0 is amplitude of the applied magnetic field, H_c is the characteristic field, $H_c = I_c/w\pi$, and $g(x)$ is given in (7).

$$g(x) = (2/x)\ln\cosh(x) - \tanh(x) \quad (7)$$

Regarding the analytical results shown in Fig. 4, $n_f Q_{BI}$ corresponds to the contribution of Q_{BI} for all filaments. The result given by $2/\pi\, n_f Q_{BI}$ has an added factor of $2/\pi$ to consider the portion of the tape that is impacted by external magnetic field considering the cable spiral structure [18]. In electrical machines, it is realistic for the armature windings to experience magnetic leakage flux densities ranging from 10 to 100 mT during standard operation [31], [32]. In these conditions, experimental and analytical results support the 2D model. In the remaining analyses, the 2D model is used for SC performance estimation as it allows calculating AC losses with reduced computational complexity and simulation time.

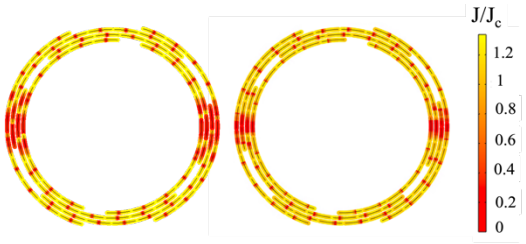

Fig. 3. Normalized current density amplitude $|\mathbf{J}|/J_c$, computed in the 2D (a) and (b) 3D SCSC cable models (B_m = 100mT).

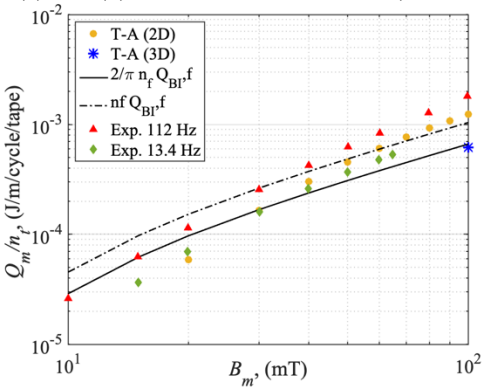

Fig. 4. Simulated magnetization loss results for SCSC cable with varying amplitude of external magnetic field and experimental results from [28].

III. AC Loss Estimation In Electrical Machine Armature Windings

The introduction of superconductor models in 3D electrical machines simulations is highly unpractical. High detail required in the tapes' mesh and the non-linearity of the material's resistivity make 3D models exceedingly demanding [33], [34]. The authors proposed in [21] a 2D model to replicate the working conditions of the superconductors in electrical machine stator coils to facilitate the SCs analyses. According to electromagnetic studies on the 3D electrical machines equipped with conventional copper conductors, the field surrounding the superconductors can be represented in a 2D cut plane of the armature slot. This means the superconductor can be analyzed with a 2D model, when the magnetic field solution obtained in 3D models is imposed through boundary conditions.

A. 2D Slot model

To apply the proposed methodology a non-optimized 10-pole 12-slot AFPM machine (shown in Fig. 5a) was designed by the authors using conventional sizing equations [35]. This topology was chosen since it can be realized with toroidal core wound coils, easily respecting the SCs bending limits. Additionally, a multi-stage structure will allow for better exploitation of the stator flux. The 3D motor study is performed with an imposed slot current of 910 A (in the 9 conducting elements) at a supply frequency of 100 Hz. The slot model methodology is illustrated in Fig. 5b. To ensure the representation of all magnetic field harmonics, the field in the armature slot is acquired at each mesh point of the slot boundaries at each time step the 3D FEM motor study solved with conventional copper conductors.

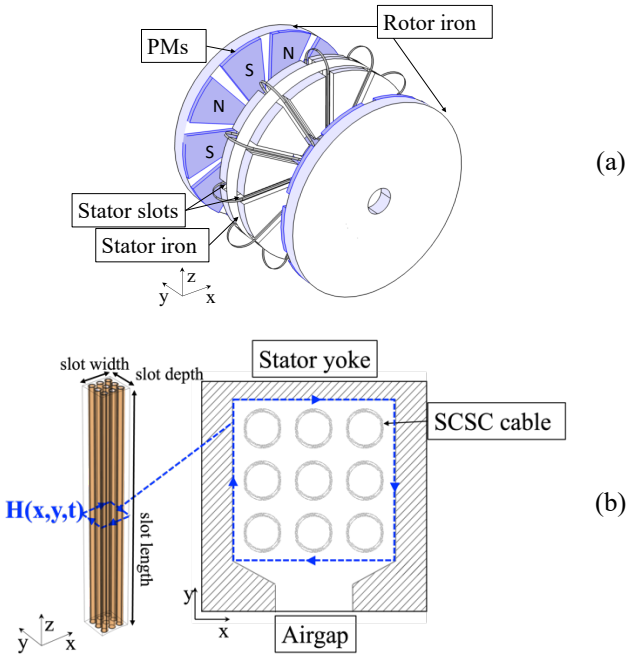

Fig. 5. 3D sketch of the 10-pole 12-slots single-stator double rotor case study AFPM machine (a) and (b) armature slot model in 3D (left) and 2D (right), the boundary for acquiring the magnetic field conditions is marked in blue dashed line.

The acquired field is imposed in a 2D model where the *T-A* formulation is applied to the superconductors to estimate their AC losses. Note that by defining the tangential component of the field along the slot borders, through Ampere's law, the total current inside the slot is also defined. This is feasible because the same current is being applied in the 3D model to the conducting elements and in 2D to the superconducting tapes.

B. Numerical simulation results

The results of the magnetic flux density color shade map |**B**| and flux density arrow surface are plotted, for the REBCO tapes and for the SCSC cables in Figs. 6a and b. In Table II are listed the estimated losses, computed by the slot model, for the SCSC cables and for SC tapes positioned parallel and perpendicularly to the machine's leakage magnetic field.

The resulting losses for the SCSC cables are higher than those calculated for the REBCO tapes when the external field is parallel to the tape's surface, and lower than those for tapes perpendicular to the external magnetic field i.e., rotated 90º relative to the position shown in Fig. 6a. Since the superconductor performance is greatly impacted by external fields perpendicular to the surfaces of the tapes and filaments, this result is expected.

In case of applied magnetic fields, SCSC cables outperform other non-spiral REBCO conductors (such as Roebel cables and twisted stacked tape cables) or single REBCO tapes since they are less affected by the direction of the applied field, resulting in low AC losses. However, when the tape surface can be arranged parallel to the magnetic field, Roebel cables or REBCO tapes may be more advantageous in terms of low AC loss and high critical current.

TABLE II
SCSC CABLES AND REBCO LOSSES COMPUTED IN THE 2D SLOT MODEL

Model	P (W/m)
SCSC Cables	4.91
REBCO tapes ∥ field	1.24
REBCO tapes ⊥ field	18.1

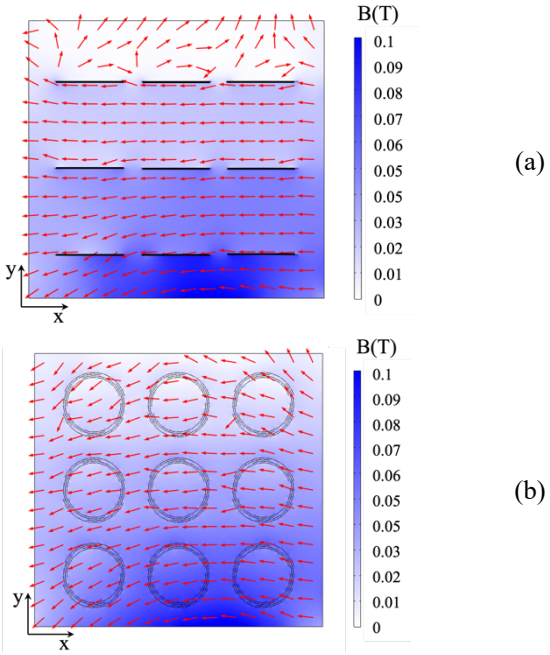

Fig. 6. Magnetic flux density color shade map and B_x, B_y surface plot arrows in the 2D slot model with the superconducting tapes parallel to the leakage field (a), and with SCSC cables (b).

IV. CONCLUSION

This paper presents a methodology to estimate losses of different superconducting tapes/cables in electrical machines' armature windings that, for their geometrical nature, require 3D simulation models. Superconducting stator coils made of SCSC cables and REBCO tapes were considered. Using the *T-A* formulation, 3D and 2D models of SCSC cables were developed and loss results were compared with experimental data in literature and analytical solutions.

The cables losses in electrical machines armature windings were analyzed for a case-study AFPM and their performance is compared to that of superconducting REBCO tapes with different orientations inside the stator slots, showing the applicability of SCSC cables in armature windings of electrical machines.

The developed modeling approach allows to restrict the FEM simulation only to the slot and the SC elements, avoiding dealing with moving mesh for the rotor and other non-linear materials, such as laminated iron cores, when superconducting elements are considered. This methodology provides an efficient procedure for loss estimation in the design of superconducting AC electrical machines, and it can be used to estimate the cooling power required for different superconducting materials in electrical machines AC windings.

REFERENCES

[1] F. Ferreira da Silva, J. F. P. Fernandes, and P. J. da Costa Branco, "Barriers and Challenges Going from Conventional to Cryogenic Superconducting Propulsion for Hybrid and All-Electric Aircrafts," *Energies*, vol. 14, no. 21, 2021, Art no. 6861.

[2] C. C. T. Chow, M. D. Ainslie, K. T. Chau, "High temperature superconducting rotating electrical machines: An overview," *Energy Reports*, vol. 9, pp. 1124-1156, 2023.

[3] M. Biasion, J. F. P. Fernandes, S. Vaschetto, A. Cavagnino and A. Tenconi, "Superconductivity and its Application in the Field of Electrical Machines," 2021 IEEE International Electric Machines & Drives Conference (IEMDC), Hartford, CT, USA, 2021, pp. 1-7.

[4] F. Gömöry, et al. "Predicting AC Loss in Practical Superconductors." *Supercond. Sci. Technol.* vol. 19, no. 3, pp. S60–S66. 2006.

[5] B.M.O. Santos, F.J.M. Dias, F. Trillaud, G.G. Sotelo, R. de Andrade Junior, "A Review of Technology Readiness Levels for Superconducting Electric Machinery," *Energies* vol. 16, 2023, Art no. 5955.

[6] H. Zhang, Z. Wen, F. Grilli, K. Gyftakis, M. Mueller, "Alternating Current Loss of Superconductors Applied to Superconducting Electrical Machines," *Energies*, vol. 14, no. 8 2021, Art no. 2234.

[7] N. Amemiya, Z. Jiang, Y. Iijima, K. Kakimoto and T. Saitoh, "Total AC loss of YBCO coated conductor carrying AC transport current in AC transverse magnetic field with various orientations," *Supercond. Sci. Technol.*, vol. 17, pp. 983, Jun. 2004.

[8] A. Wolfbrandt, N. Magnusson and S. Hornfeldt, "Losses in a BSCCO/Ag tape carrying AC transport currents in AC magnetic fields applied in different orientations," *IEEE Trans. Appl. Supercond.*, vol. 11, no. 4, pp. 4123-4127, Dec. 2001.

[9] S. Fukui, J. Ogawa, J. Takahashi, Y. Kobu, T. Sato and T. Nakamura, "Study on AC Loss Characteristics of 3-Phase HTS Coils With Iron Core and Its Reduction," *IEEE Trans. Appl. Supercond.*, vol. 29, no. 5, pp. 1-5, Aug. 2019, Art no. 8201305.

[10] Y. Zhang, Y. Cheng, R. Qu, D. Li, Y. Gao and Q. Wang, "AC Loss Analysis and Modular Cryostat Design of a 10-MW High-Temperature Superconducting Double Stator Flux Modulation Machine," *IEEE Trans. Ind. Appl.*, vol. 58, no. 6, pp. 7153-7162, Dec. 2022.

[11] R. Mellerud, C. Hartmann, C. L. Klop, S. Austad and J. K. Nøland, "Design of a Power-Dense Aviation Motor with a Low-Loss Superconducting Slotted Armature," *IEEE Trans. Appl. Supercond.*, vol. 33, no. 8, pp. 1-13, Nov. 2023, Art no. 5204013.

[12] W. J. Carr and C. E. Oberly, "Filamentary YBCO conductors for AC applications," *IEEE Trans. Appl. Supercond.*, vol. 9, no. 2, pp. 1475-1478, June 1999.

[13] N. Amemiya, S. Kasai, K. Yoda, Z. Jiang, G. A. Levin, P. N Barnes and C. E. Oberly, "AC loss reduction of YBCO coated conductors by multifilamentary structure," *Supercond. Sci. Technol.* vol.17, pp. 14641471, 2004.

[14] S. You, S. S. Kalsi, M. D. Ainslie, R. A. Badcock, N. J. Long and Z. Jiang, "Simulation of AC Loss in the Armature Windings of a 100 kW All-HTS Motor With Various (RE)BCO Conductor Considerations," *IEEE Access*, vol. 9, pp. 130968-130980, 2021.

[15] M. Shigemasa, Y. Sogabe, N. Wang, A. Takahashi, and N. Amemiya, "Impact of Copper Thickness, Conductor Width, and Number of Striations on Coupling Loss Characteristics of Copper-Plated Multifilament-Coated Conductors," *IEEE Trans. Appl. Supercond.*, vol. 32, pp. 1–12 2022.

[16] N. Amemiya, Y. Zhao, X. Luo, G. Xu, Y. Li, and Y. Sogabe, "Current Sharing Between Filaments and Voltage – Current Characteristics of Copper-Plated Multifilament Coated Conductors," *IEEE Trans. Appl. Supercond.*, vol. 32, no. 6, pp. 1-5, Sept. 2022, Art no. 8001005.

[17] F. Grilli and A. Kario, "How filaments can reduce AC losses in HTS coated conductors: a review," *Supercond. Sci. Technol.* vol. 29, 2016, Art no. 083002.

[18] N. Amemiya et al. "Effective Reduction of Magnetization Losses in Copper-Plated Multifilament Coated Conductors Using Spiral Geometry." *Supercond. Sci. Technol.* vol. 35, pp. 25003, 2022.

[19] Y. Sogabe, Y. Mizobata, and N. Amemiya. "Coupling Time Constants and Ac Loss Characteristics of Spiral Copper-Plated Striated Coated Conductor Cables (SCSC Cables)," *Supercond. Sci. Technol.*, vol. 33.5, pp. 55008, 2020.

[20] D. J. Gameiro Carvalho, F. Ferreira da Silva, J. F. P. Fernandes and P. J. da Costa Branco, "Finite-element recipes for HTS-coated conductors and HTS tape topologies," *Supercond. Sci. Technol.*, vol. 36, no. 10, 2023.

[21] I. S. P. Peixoto, S. Vaschetto, J. F. P. Fernandes, P. J. Da Costa Branco, A. Tenconi and A. Cavagnino," Modeling Approach for Superconducting AC Windings: Case Study on Axial Flux PM Machines," 2023 IEEE Energy Conversion Congress and Exposition (ECCE), Nashville, TN, USA, 2023, pp. 3790-3795.

[22] H. Tsuboi, and K. Kunisue, "Eddy Current Analysis of Thin Plates Taking Account of the Source Current Distributions and Its Experimental Verifications," *IEEE Trans. Magn.,* vol.27 pp. 4020–4023, 1991.

[23] M. Nii, N. Amemiya, and T. Nakamura, "Three-Dimensional Model for Numerical Electromagnetic Field Analyses of Coated Superconductors and Its Application to Roebel Cables," *Supercond. Sci. Technol.* vol. 25 pp. 95011, 2012.

[24] D. X. Chen; R. B. Goldfarb, "Kim model for magnetization of type-II superconductors," *J. Appl. Phys*., vol. 66, pp. 2489–2500, 1989.

[25] D. A. Cardwell, D. C. Larbalestier, A. Braginski, Handbook of Superconductivity: Characterization and Applications, 2nd ed., vol. 3 CRC Press, 2022

[26] F. Huber et al., "The T-A formulation: an efficient approach to model the macroscopic electromagnetic behaviour of HTS coated conductor applications," *Supercond. Sci. Technol.*, vol. 35, pp. 043003, 2022.

[27] E. Berrospe-Juarez, et al., "Real-Time Simulation of Large-Scale HTS Systems: Multi-Scale and Homogeneous Models Using the T-A Formulation." *Supercond. Sci. Technol.* vol.32 pp. 65003, 2019.

[28] M. Shigemasa, Y. Sogabe, A. Takahashi and N. Amemiya, "Impact of Number of Layers on Magnetization Losses of Spiral Copper-Plated Multifilament Coated Conductors," *IEEE Trans. Appl. Supercond.*, vol. 33, no. 5, pp. 1-6, Aug. 2023, Art no. 5901406.

[29] Y. Yan, P. Song, W. Li, J. Sheng, and T. Qu, "Numerical Investigation of the Coupling Effect in CORC Cable With Striated Strands," *IEEE Trans. Appl. Supercond.*, vol. 30, no. 4, pp. 1-5, June 2020, Art no. 4800305.

[30] E. H. Brandt, and M. Indenbom, "Type-II-superconductor strip with current in a perpendicular magnetic field," *Phys. Rev. B*, vol. 48, pp. 12893–12906, Nov. 1993.

[31] L. F. D. Bucho, F. F. da Silva, J. F. P. Fernandes and P. J. C. Branco, "Electromechanical Analysis of HTS Cage Rotors for Induction-Synchronous Machines," *IEEE Trans. Appl. Supercond*, vol. 34, no. 3, pp. 1-5, May 2024, Art no. 5201805.

[32] N. Arish, "Leakage flux reduction of axial-flux switching PM machine by using HTS-disk", *Physica C: Superconductivity and its Applications*, vol. 590, 2021.

[33] L. Hao, F. Dong, J. Hu et al. "3D Electromagnetic Modelling for High temperature Superconducting Dynamo Flux Pumps Using T-A Formulation," *High voltage*, 1–13, 2024.

[34] I. S. P. Peixoto, F. F. da Silva, J. F. P. Fernandes, S. Vaschetto and P. J. C. Branco, "A Distributed Equivalent-Permeability Model for the 3-D Design Optimization of Bulk Superconducting Electromechanical Systems," *IEEE Trans. Appl. Supercond.*, vol. 33, no. 6, pp. 110, Sept. 2023, Art no. 3601610.

[35] S. Vaschetto, A. Tenconi and G. Bramerdorfer, "Sizing procedure of surface mounted PM machines for fast analytical evaluations," 2017 IEEE International Electric Machines and Drives Conference (IEMDC), Miami, FL, USA, 2017, pp. 1-8.